

ORIGINAL ARTICLE

Effect of Ammonia on the Synthesis of NMC541 Cathode Materials with the Sol-Gel Method

Y. Purwamargapratala^{1,2*}, J. F. Safitri³, E. B. Nursanto³, H. Jodi², E. Kartini² and A. Zulfia¹

¹Department of Metallurgy and Material Engineering, University of Indonesia

²National Research and Innovation Agency, Indonesia

³Pertamina University, Jakarta, Indonesia

ABSTRACT – The research studied about the effect of ammonia on the synthesis of lithium-ion battery cathode materials $\text{LiNi}_{0.5}\text{Mn}_{0.4}\text{Co}_{0.1}\text{O}_2$ (NMC541) through a sol-gel method by modifying the mole ratio of ammonia to metal forming ratios (0.5; 1.0; 1.5; and 2.0). The precipitation formed at pH 11 and at temperature of 80°C. Characterization was carried out on samples resulting from pyrolysis (pyrolysis result), with calcination for once and twice at 850°C for 3 hours, X-ray diffraction pattern characterization, morphological characterization using scanning electron microscope (SEM), and conductivity characterization using an impedance capacitance conductance (LCR) meter. The result of the synthesis is in the form of spherical particles. The addition of ammonia affected the particle size distribution and stoichiometry of the metal forming NMC541, even though it was not significant. The ammonia to metal ratio of 1.5 (Sample N1.5-K) resulted in the distribution with the optimum particle homogeneity. The morphology of the pyrolysis and 3 hours-850°C calcined samples was dominated by spherical particles and agglomeration. Particle growth in the material is affected by heat treatment time. Samples with ammonia to metal ratio of 2.0 (N2.0-K) have the closest stoichiometry to NMC541. The total conductivity of the sample at a measurement frequency of 42Hz-1MHz is in the value range of 10^{-7} – 10^{-5} S.cm⁻¹. The particle size is also affected by the calcination temperature. The effect of using ammonia in the synthesis process is not directly related to the electrical properties. However, it is related to the purity of NMC541. Samples of N1.5-K pyrolyzed result and samples of N1.0-K (3 hour 850 °C calcined) have optimum conductivity values. Agglomeration as a calcination effect lowers the conductivity value. The addition of 3 hours of calcination time does not significantly increase the conductivity value.

ARTICLE HISTORY

Received: 12 Oct 2022

Revised: 28 Oct 2022

Accepted: 31 Oct 2022

KEYWORDS

NMC541

Sol-gel

Ammonia

Conductivity

INTRODUCTION

The lithium-ion battery is one type of secondary battery which can be recharged and used repeatedly. Battery is composed of a cathode, anode, separator, and electrolyte [1]. Optimization of a battery can be done on cathode, anode, and separator materials [2]–[4]. There are several cathode materials commonly used, including LiMn_2O_4 , LiFePO_4 , LiNiMnCoO_2 , and LiNiCoAlO_2 [2]. $\text{LiNi}_x\text{Mn}_y\text{Co}_{1-x-y}\text{O}_2$ (NMC) is one of the successful material for energy storage by producing excellent specific power performance, long life cycle, cost-friendly, more safety, and superior specific energy levels derived from nickel-manganese-cobalt synergies [5]. Variation in mole composition between Ni, Mn, and Co are different, for instance $\text{LiNi}_{0.1}\text{Mn}_{0.1}\text{Co}_{0.1}\text{O}_2$ (NMC111), $\text{LiNi}_{0.4}\text{Mn}_{0.4}\text{Co}_{0.2}\text{O}_2$ (NMC442), $\text{LiNi}_{0.5}\text{Mn}_{0.3}\text{Co}_{0.2}\text{O}_2$ (NMC532), $\text{LiNi}_{0.5}\text{Mn}_{0.4}\text{Co}_{0.1}\text{O}_2$ (NMC541), and $\text{LiNi}_{0.8}\text{Mn}_{0.1}\text{Co}_{0.1}\text{O}_2$ (NMC811) [6].

The composition of NMC541 has the smallest contraction of structural expansion during the cycle and has the best structural stability at high stresses [6]. The measurement of conductivity values was obtained by TODA America Inc. on $\text{LiNi}_{0.3}\text{Mn}_{0.3}\text{Co}_{0.3}\text{O}_2$ (NMC333) and NMC532, which has been sintered at 900°C for 12 hours, to produce a conductivity value of 9.1×10^{-9} S.cm⁻¹ for NMC333 and 8.7×10^{-9} S.cm⁻¹ for NMC532. Optimization of the synthesis conditions for NMC532 has been done, one of which was by varying the mole ratio of NH_3 to metal sulfate (0.8; 0.4; 1.5; and 2.5), showing significant differences in size, shape, and particle distribution [7].

The commonly used synthesis methods to produce $\text{LiNi}_x\text{Mn}_y\text{Co}_{1-x-y}\text{O}_2$ include coprecipitation [8], sol-gel [3], solid state [9], and hydro-thermal [10]. The synthesis of NMC111 using the sol-gel method shows fine crystal formation with particle size of 100–200 nm and has good performance [11]. The sol-gel method for the synthesis of $\text{Li}_4\text{Ti}_5\text{O}_{12}$ (LTO) anode material as an anode also produces 99% purity which is much better than the 57% purity value of commercial LTO with smaller particle size [3]. The conductivity value of Li-rich NMC can be affected by the amount of use of ionic liquid (IL). The higher mass of IL, the higher conductivity value, 20wt.% IL= 2.9×10^{-7} S.cm⁻¹ and 70 wt.% IL= 1.1×10^{-3} S.cm⁻¹ [12].

This study reports the effect of ammonia on the synthesis of the cathode material $\text{LiNi}_{0.5}\text{Mn}_{0.4}\text{Co}_{0.1}\text{O}_2$ (NMC541) with variations in the mole ratio of ammonia to the metal forming NMC541. Ammonia is needed in the formation of sol-gel. In order that, it is necessary to determine the optimal ratio of ammonia concentration to the metals forming NMC541.

*CORRESPONDING AUTHOR | Y. Purwamargapratala | ✉yustinus.purwamargapratala@ui.ac.id ; yust002@brin.go.id

The conductivity of the material was characterized using an impedance capacitance conductance (LCR) meter. Furthermore, X-ray diffractometer is used to determine the phase and crystal size, as well as the crystallinity of the material. Scanning electron microscopy (SEM) is utilized to see the morphology and homogeneity of particles in the material [13].

EXPERIMENTAL METHOD

$\text{LiNi}_{0.5}\text{Mn}_{0.4}\text{Co}_{0.1}\text{O}_2$ were synthesized by sol-gel method with the addition of ammonia as a gelling agent. The synthesis procedure includes three steps: the sol-gel formation process, the pyrolysis process, and the calcination process. Acetate salts of $\text{Ni}(\text{CH}_3\text{COO})_2 \cdot 4\text{H}_2\text{O}$ (98%, Aldrich), $\text{Mn}(\text{CH}_3\text{COO})_2 \cdot 4\text{H}_2\text{O}$ (99.99%, Sigma-Aldrich), and $\text{Co}(\text{CH}_3\text{COO})_2 \cdot 4\text{H}_2\text{O}$ (Merck) were dissolved in aquabidest and NaOH was added as a chelating agent (1:1 mole ratio). The acidity adjusted by the addition of ammonia (28–30%, Sigma-Aldrich) until the pH value is 11. The resulting slurry is then filtered, washed using aquabidest, dried in an oven at 80°C , and mixed with LiOH ($\geq 98\%$, Sigma-Aldrich) (mole ratio 1:1) and ammonia with various mole ratio (1:0.5; 1:1; 1:1.5; and 1:2). The solution was stirred at 80°C to form a gel. The gel was dried through a pyrolysis process at 450°C for 5 hours to remove organic matter. The obtained precursor was then calcined at 850°C for 3 hours. The resulting $\text{LiNi}_{0.5}\text{Mn}_{0.4}\text{Co}_{0.1}\text{O}_2$ samples were further characterized by X-ray diffractometer (XRD) (PanAnalytical Empyrean), using $\text{CuK}\alpha$ beam operated at 40kV and 30 mA corresponding to the X-ray wavelength of 1.5406\AA , in the range of 2θ of $10\text{--}80^\circ$. Morphological analysis of the samples were observed using scanning electron microscopy (SEM) (JSM-6510LA, JEOL) operated at 20 kV. Samples in the form of pellets were tested using impedance capacitance conductance (LCR) meter (HIOKI 3538-50 LCR HiTester) to determine the conductivity value. Each sample's name has their own meaning. N0.5-PK, N stands for ammonia, 0.5 for the mole ratio of ammonia, PK stands for pre calcinated. After calcination N0.5-PK will be named as N0.5-K; N1.0-PK will be named as N1.0-K, and so on.

RESULT AND DISCUSSION

The synthesized material was characterized using X-ray diffractometer to determine the crystal phase. Figure 1 is the diffraction pattern of the pyrolysis $\text{LiNi}_{0.5}\text{Mn}_{0.4}\text{Co}_{0.1}\text{O}_2$ (NMC541) material. All variations show the same diffraction pattern.

The diffraction pattern of the NMC541 material which has been calcined for 3 hours is shown in Figure 2, while Figure 3 shows the detail one with the crystal lattice exemplified by the N1.0-K sample. The patterns were analyzed using RIETVELD method showing the similarity of the diffraction pattern for all samples, in terms of the angular position of the peaks. The most dominant peak is at an angle of 18° , as well as the second dominant peak is at an angle of 44.3° . There are no new peaks or other peaks are formed in this diffraction pattern which means no contaminants and impurities in the sample. NMC single crystals with grain size of $2\text{--}5\ \mu\text{m}$ has good electrochemical performance thus the synthesis can be concluded to be successful [14].

The results of the refinement diffraction pattern data using RIETVELD method to determine the crystal structure of the samples are shown in Table 1. The hexagonal structure (space group: R-3m) is observed for all samples without impurities. Comparison of the intensity on miller index (003) and (104), (I003/I104), is the main indicator of the degree of cation mixing [15]. The mixing of Ni^{2+} and Li^+ ions is caused by the size of the ionic radii which is almost the same, ($r_{\text{Ni}^{2+}} = 0.69\text{\AA}$) and ($r_{\text{Li}^+} = 0.76$). The ions mixing will slow down the diffusivity of Li ions and reduce the electrochemical performance of a battery. When $\text{I003/I104} > 1.2$, it indicates a low degree of cation mixing [16].

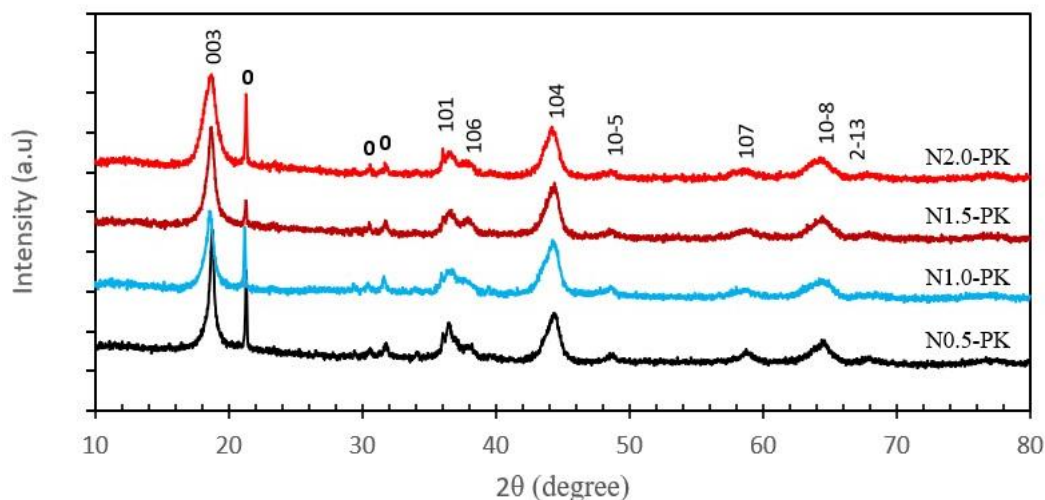


Figure 1. Diffraction pattern of NMC541 results in pyrolysis (before calcination)

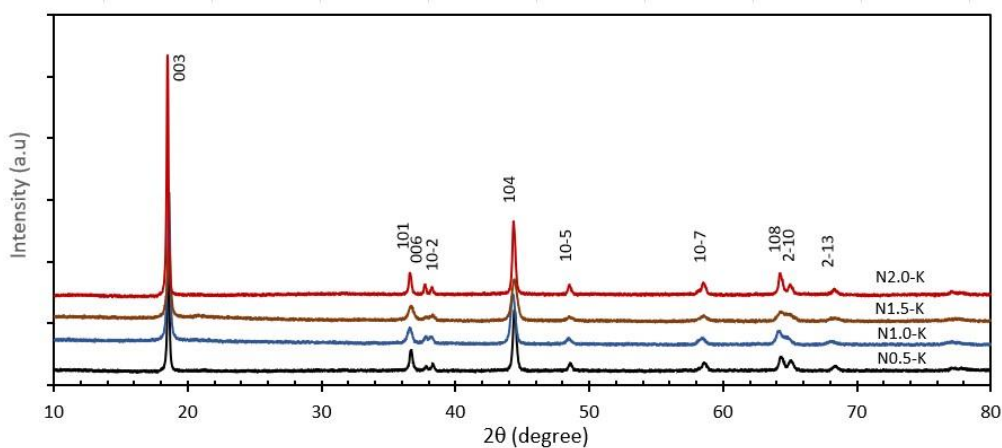


Figure 2. NMC541 diffraction pattern after calcination at 800°C for 3 hours

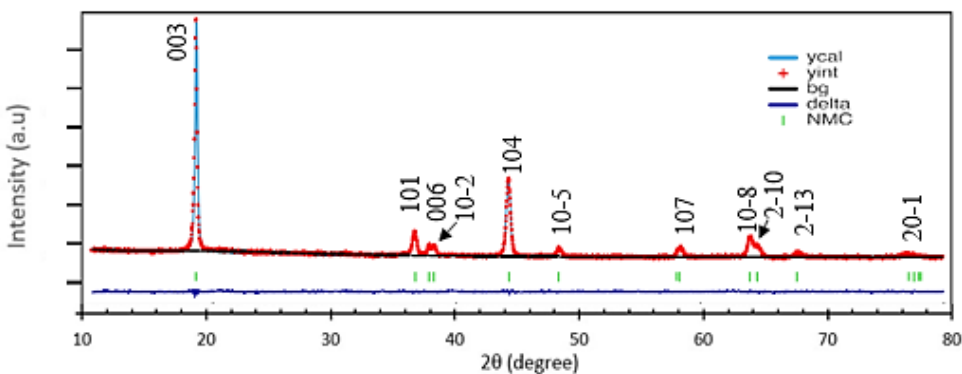


Figure 3. N1.0K diffraction pattern after 3 hours calcination

The lattice parameter value can be related to the Mn or Co mixing in Ni which can increase the concentration of Ni²⁺ from the equivalence of cations and anions in NMC541 [15]. The c/a values of all samples showed almost the same results. It indicates that by varying the concentration of ammonia, the NMC crystal structure will still formed.

Table 1. Comparison of NMC541 lattice parameters with variation in mole ratio of ammonia to metals acetat samples (0.5; 1.0; 1.5; 2.0).

Code	a (Å)	c (Å)	c/a	I ₀₀₃ /I ₁₀₄	D (nm)
N0.5-K	2.872	14.269	4.968	1.782	40.29
N1.0-K	2.878	14.280	4.962	2.990	29.94
N1.5-K	2.866	14.253	4.973	1.758	24.36
N2.0-K	2.872	14.269	4.968	3.245	47.65

The X-ray diffraction pattern of the NMC541 sample which calcined twice for 3 hours are shown in Figure 4. The diffraction pattern for those samples shows a similar pattern as the sample which calcined once for 3 hours. However, in sample N0.5-K2 gives a new diffraction peak at 2θ angle of 31° which can be attributed to the presence of contaminants.

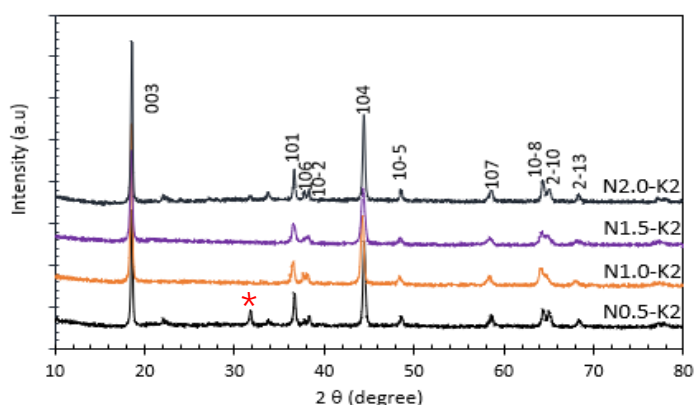


Figure 4. NMC541 diffraction pattern after twice calcination at 850°C for 3 hours

Characterization of NMC541 using SEM has been carried out to determine the distribution of the synthesized particles through the sol-gel method. Figure 5 shows morphological picture of the NMC541 samples with variations in the mole ratio of ammonia to its constituent metals, pyrolysis results. From the result, it can be shown that the samples are generally formed by particles of spherical shape and several agglomerates of various sizes. Moreover, it can be seen that the N1.5-PK sample has a fairly homogeneous distribution. Meanwhile, in samples with other ammonia variations, the particles agglomerate more and some of the shapes resembled flakes.

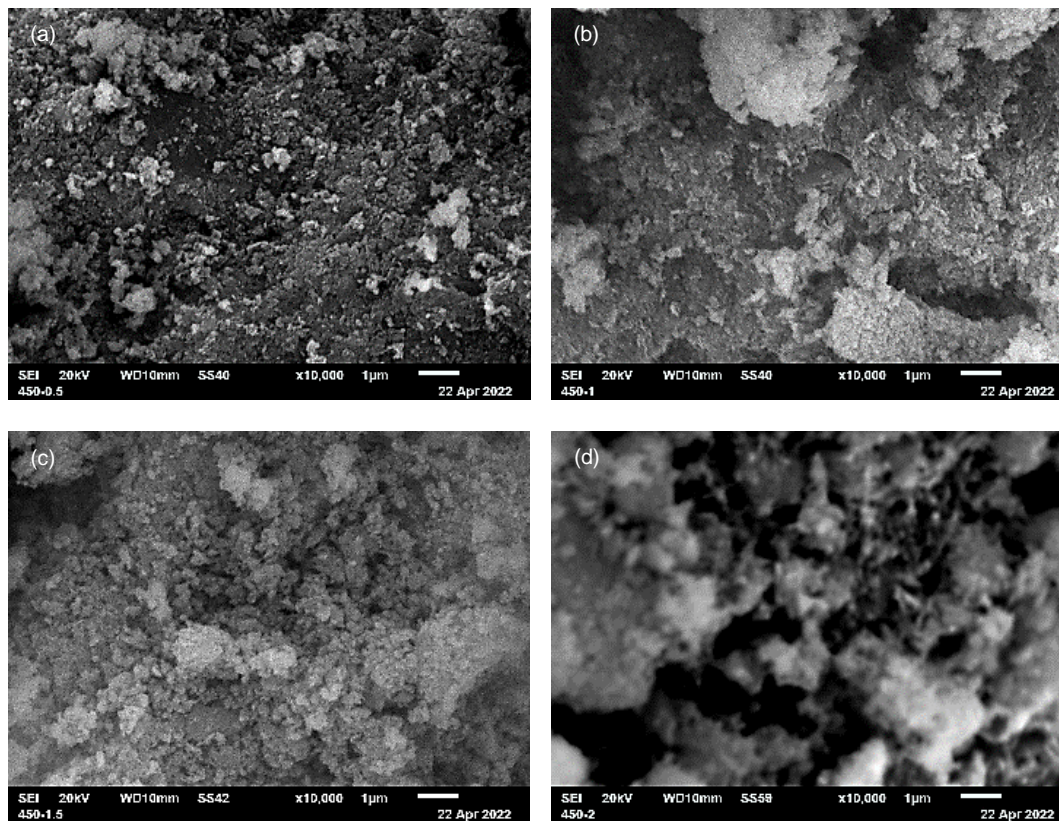


Figure 5. Morphology of pyrolysis NMC541 particles in ratio of ammonia/Mac variation: (a) N0.5-PK, (b) N1.0-PK, (c) N1.5-PK, and (d) N2.0-PK

The morphology of the NMC541 sample calcined at 850°C for 3 hours by SEM characterization are shown in Figure 6. From the figure, it is known that the morphology of the samples were dominated by spherical particles and agglomeration, as well as the morphology of the pyrolysis samples. However, the size of the agglomeration looks larger than the pyrolysis results, which is probably due to some of the sample particles agglomerated at high temperatures calcination. The N1.0-K sample appears to have more homogeneous particle distribution and size when compared to other samples. SEM observation of samples N0.5-K and N1.5 K show that the particle distribution was less homogeneous and there were agglomerated particles. Meanwhile, sample N2.0-K shows the average particle agglomeration. The diversity of particle sizes would greatly affect the electrical properties of the material, particularly in its conductivity. A certain level of inhomogeneity can increase the conductivity of the material. On the other hand, a very high inhomogeneity can cause the charge carriers in the material to be more difficult to move which result in a decrease in conductivity [17]. N2.0-K showed that the particle distribution was less homogeneous and there were agglomerated particles.

Particle size can affect the specific capacity of a sample. The smaller the particle size, the more specific capacity will increase [18]. The growth of particles in the material is strongly influenced by the time used to provide heat treatment. A long heat treatment time will provide sufficient time for the particles to move and make agglomerates evenly [19]. In addition, the particle size is also influenced by the temperature during calcination, where the higher the temperature, the faster the agglomerate growth [20].

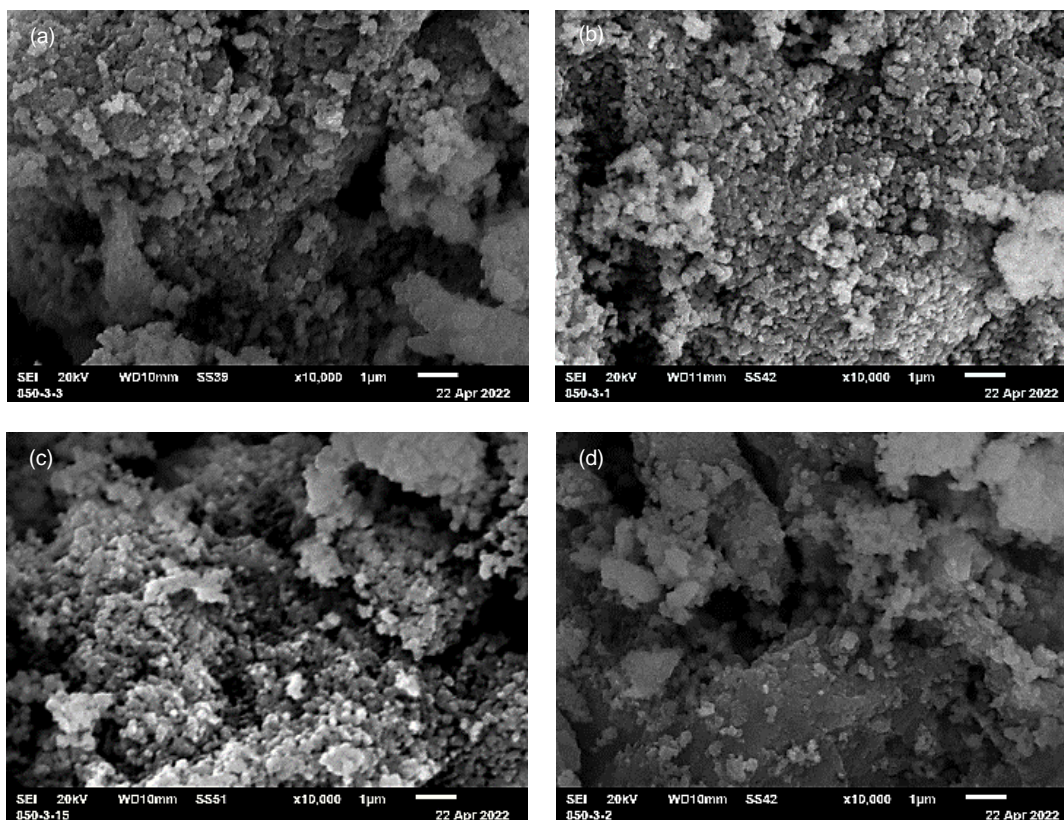


Figure 6. NMC541 particle morphology after calcination in ammonia variation:(a) N0.5-K, (b) N1.0-K, (c) N1.5-K, and (d) N2.0-K

Table 2 shows the composition of each material tested using energy dispersive X-ray (EDX). N2.0-K sample shows a composition value which is the closest one to the expected value of 541. Meanwhile, the composition of the other variations showed that the Mn fraction is higher than Ni [21].

Table 2. Composition of NMC541 EDX test results

Sample Code	Before Calcination (450°C)			Sample Code	After Calcination (850°C)		
	Ni	Mn	Co		Ni	Mn	Co
N0.5-PK	3.94	4.16	1.00	N0.5-K	4.52	5.39	1.00
N1.0-PK	3.99	5.41	1.00	N1.0-K	4.83	5.71	1.00
N1.5-PK	3.32	5.59	1.00	N1.5-K	3.83	5.57	1.00
N2.0-PK	6.06	4.47	1.00	N2.0-K	5.68	5.54	1.00

Figure 7 shows a plot of the sample conductivity against the measurement frequency obtained from the sample impedance measurement at room temperature in the frequency range of 42 Hz–1 MHz. It shows that the total conductivity of all samples is in the same value range, which is between 10^{-7} – 10^{-5} S.cm⁻¹. From the total conductivity curve, the DC conductivity value of the material can be obtained, which is a value that represents the electrical properties of the material by fitting the measurement curve to the universal conductivity formula, called Jonscher universal power law [22]. Changes in DC conductivity value of each sample are depicted in the insert image in Figure 7 and compiled in Figure 8, while the values are listed in Table 2.

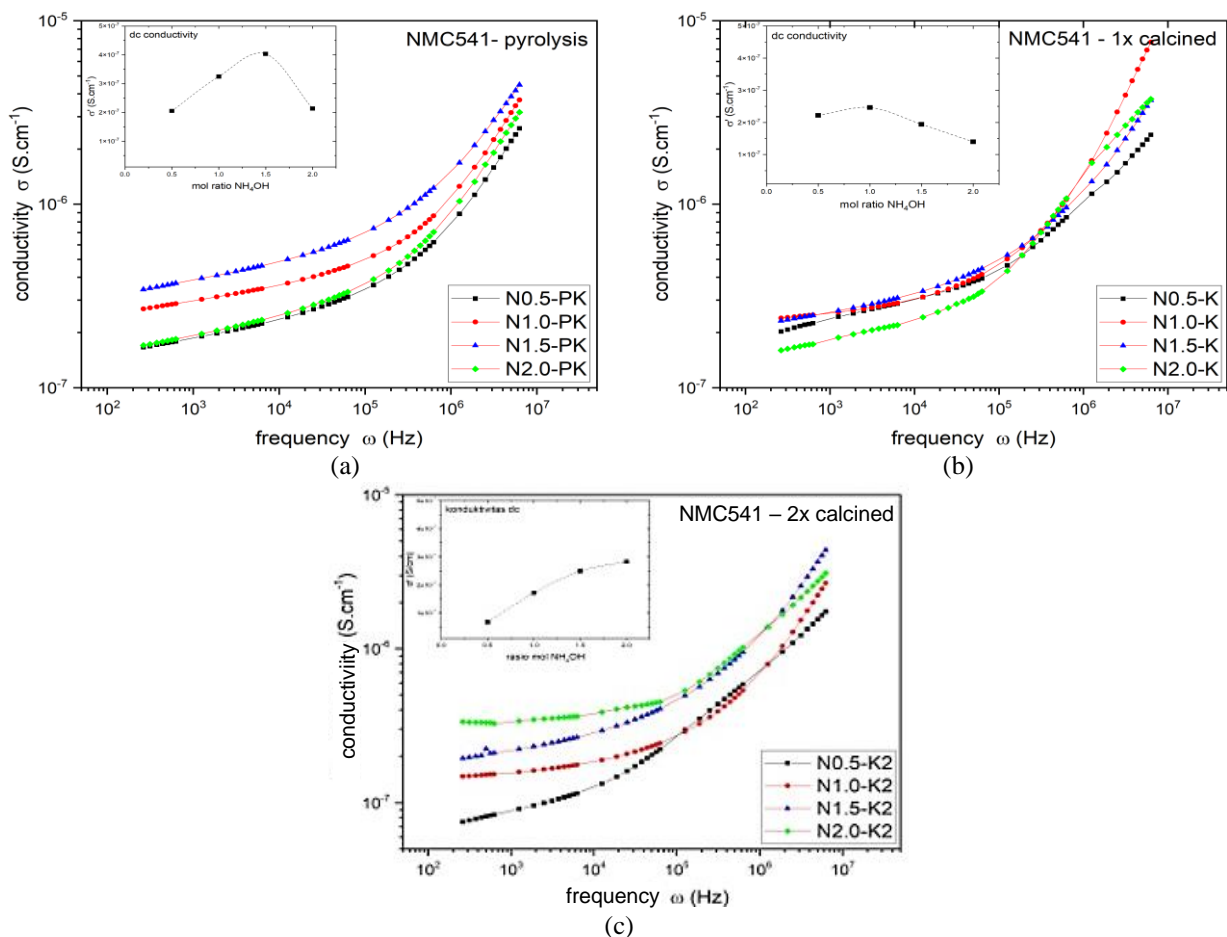


Figure 7. The conductivity curve of the NMC541 sample as a function of measurement frequency and the DC conductivity curve (insertion image): (a) NMC 541 pyrolysis results, (b) NMC541-1x calcination, and (c) NMC541-2x calcination

Table 3. The DC conductivity value of NMC451 samples

No	Sample code	Ammonia/Mac	DC Conductivity (S.cm ⁻¹)
NMC541–pyrolysis result			
1	N0.5-PK	0.5	2.051×10 ⁻⁷
2	N1.0-PK	1.0	3.246×10 ⁻⁷
3	N1.5-PK	1.5	4.033×10 ⁻⁷
4	N2.0-PK	2.0	2.130×10 ⁻⁷
NMC541–once calcination			
5	N0.5-K	0.5	2.217×10 ⁻⁷
6	N1.0-K	1.0	2.462×10 ⁻⁷
7	N1.5-K	1.5	1.940×10 ⁻⁷
8	N2.0-K	2.0	1.397×10 ⁻⁷
NMC541–twice calcination			
9	N0.5-K2	0.5	6.703×10 ⁻⁸
10	N1.0-K2	1.0	1.712×10 ⁻⁷
11	N1.5-K2	1.5	2.489×10 ⁻⁷
12	N2.0-K2	2.0	2.826×10 ⁻⁷

To know the effect of calcination time to the conductivity value of the material, a further calcination process was carried out, twice for 3 hours. From Figure 8, it can be seen that the conductivity of NMC541 which underwent calcination both once and twice for 3 hours have a lower value than the conductivity of the pyrolysis NMC541. As already discussed in the discussion of morphology, calcination at high temperature can affect the movement of particles to form agglomeration in the sample. The presence of agglomeration in the sample creates inhomogeneities in the sample which can decrease the conductivity value. The inhomogeneities in the material due to the presence of other phases and impurities which give the composite effect, at controlled levels, can have a favorable effect on the electrical properties [23]. However, if the level is not controlled, the effect will be otherwise.

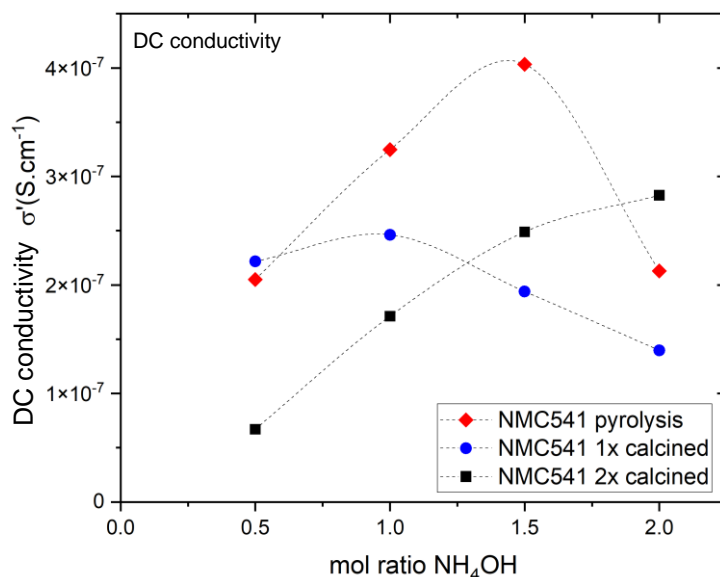


Figure 8. Graph of DC conductivity of NMC541 pyrolysis sample (without calcination) vs. calcined

The conductivity values of all samples are on the same order which means the effect of using ammonia in the synthesis process is not directly related to the electrical properties. However, it is directly related to the quality of the synthesis product, namely the purity of NMC541 as shown by the results of XRD analysis. The difference in conductivity values seems to be directly related to the result of imperfect calcination treatment which creates inhomogeneity in the material. As can be seen from the SEM morphology, samples with good homogeneities, such as the N1.5-PK sample (without calcination) and the N1.0-K (after calcination) sample (3 hours calcined), have the optimum conductivity values in their group, compared to other samples containing more agglomeration. The presence of agglomeration due to the calcination effect seems to reduce the conductivity value, which is probably due to the incomplete agglomeration process. The addition of calcination time for the next 3 hours has not yet increased the conductivity value, which is a possible coarse composite effect (the ratio between particles to agglomerates) still does not show the ideal composition. The addition of a longer calcination time is expected to give more time for all particles to move and form ideal agglomeration which will result in improvement of conductivity properties in the material. However, as can be seen in Figure 8, the addition of calcination time has a good effect on the change in the conductivity of the sample, as the mole ratio of ammonia used in the synthesis process increases. At the ammonia mole ratio of 2.0, the DC conductivity value of the sample with a longer calcination time shows the best conductivity.

CONCLUSION

The results of $\text{LiNi}_{0.5}\text{Mn}_{0.4}\text{Co}_{0.1}\text{O}_2$ (NMC541) synthesized by sol-gel method is in the form of spherical particles. The addition of ammonia affected the particle size distribution and composition of the metal-forming NMC541, although not significant. When the ratio of ammonia to metal is 1:1.5, resulting the most optimum particle homogeneity. The morphology of the pyrolysis and 3-hour calcination samples were dominated by spherical particles and agglomerations. The growth of particles in the material is affected by the time of heat treatment. The total conductivity of the sample at a measurement frequency of 42 Hz–1 MHz is in the value range of 10^{-7} – 10^{-5} S.cm⁻¹. The particle size is also affected by the calcination temperature, agglomerations in the sample create inhomogeneities in the sample which can reduce the conductivity value. The effect of using ammonia on the synthesis process is not directly related to the electrical properties but is related to the purity of NMC541. The addition of 3 hours calcination time does not increase the conductivity value. The addition of a longer calcination time is expected to give time for all particles to move and form ideal agglomerations which will result in conductivity improvement in the material. At an ammonia mole ratio of 2.0, the DC conductivity value of the sample with a longer calcination time gives the optimum conductivity value.

ACKNOWLEDGEMENT

The authors stated that there was no conflict of interest in the process of writing this paper and would like to express the deepest gratitude, particularly to the National Research and Innovation Agency which has greatly contributed to the funding of this research, as well as to all colleagues at the Advanced Materials Research Center and the Department of Metallurgy and Material Engineering, University of Indonesia, for the help in the form of useful advice and suggestions.

REFERENCES

- [1] Y. Purwamargapratala, Sudaryanto, and F. Akbar. "Neutron tomography study of a lithium-ion coin battery." *J. Phys.: Conf. Ser.*, vol. 1436, no. 1, p. 012029, 2020.

- [2] M. K. Tran, A. Dacosta, A. Mevawalla, S. Panchal, and M. Fowler, “Comparative study of equivalent circuit models performance in four common lithium-ion batteries: LFP, NMC, LMO, NCA.” *Batteries*, vol. 7, no. 3, p. 51, 2021.
- [3] Y. Purwamargapratala, A. Sujatno, Y. L. Sabayu, and E. Kartini, “Synthesis of $\text{Li}_4\text{Ti}_5\text{O}_{12}$ (LTO) by sol-gel method for lithium-ion battery anode.” *IOP Conf. Series: Materials Science and Engineering*, vol. 553, no. 1, p. 012062, 2019.
- [4] A. Li, A. C. Y. Yuen, W. Wang, I. M. De Cachinho Cordeiro, C. Wang, T. B. Y. Chen, J. Zhang, Q. N. Chan, and G. H. Yeoh. “A review on lithium-ion battery separators towards enhanced safety performances and modelling approaches.” *Molecules*, vol. 26, no.2, p. 478, 2021.
- [5] M. Malik, K. H. Chan, and G. Azimi, “Review on the synthesis of $\text{LiNi}_x\text{Mn}_y\text{Co}_{1-x-y}\text{O}_2$ (NMC) cathodes for lithium-ion batteries.” *Materials Today Energy*, vol. 28, p. 101066, 2022.
- [6] D. Goonetilleke, N. Sharma, W. K. Pang, V. K. Peterson, R. Petibon, J. Li, and J. R. Dahn. “Structural evolution and high-voltage structural stability of $\text{Li}(\text{Ni}_x\text{Mn}_y\text{Co}_z)\text{O}_2$ electrodes.” *Chem. Mater.*, vol. 31, no. 2, pp. 376–386, Jan. 2019.
- [7] M. Noh and J. Cho, “Optimized synthetic conditions of $\text{LiNi}_{0.5}\text{Co}_{0.2}\text{Mn}_{0.3}\text{O}_2$ cathode materials for high rate lithium batteries via co-precipitation method.” *J. Electrochem. Soc.*, vol. 160, no. 1, pp. A105–A111, 2013.
- [8] A. L. Lipson, J. L. Durham, M. LeResche, I. Abu-Baker, M. J. Murphy, T. T. Fister, L. Wang, F. Zhou, L. Liu, K. Kim, and D. Johnson. “Improving the thermal stability of NMC 622 Li-ion battery cathodes through doping during coprecipitation.” *ACS Appl. Mater. Interfaces*, vol. 12, no. 16, pp. 18512–18518, 2020.
- [9] Y. Purwamargapratala, I. Gunawan, D. N. Haerani, Sudirman, E. Kartini A. Zulfia, and A. Glushenkov. “Effect of sodium in $\text{LiNi}_{0.5}\text{Mn}_{0.3}\text{Co}_{0.2}\text{O}_2$ as a lithium ion battery cathode material by solid state reaction method.” *Journal of Fibers and Polymer Composites*, vol. 1, pp. 66–72, 2022.
- [10] Y. Xiang, M. Huang, Y. Jiang, S. Liu, J. Li, J. Wu, Z. Liu, L. Zhu, X. Wu, Z. He, and L. Xiong. “Ionic liquid assisted hydrothermal synthesis of $0.5\text{Li}_2\text{MnO}_3 \cdot 0.5\text{LiNi}_{0.5}\text{Mn}_{0.5}\text{O}_2$ for lithium-ion batteries.” *Journal of Alloys Compounds.*, vol. 864, p. 158177, 2021.
- [11] J. Xu, S. L. Chou, Q. F. Gu, H. K. Liu, and S. X. Dou. “The effect of different binders on electrochemical properties of $\text{LiNi}_{1/3}\text{Mn}_{1/3}\text{Co}_{1/3}\text{O}_2$ cathode material in lithium-ion batteries.” *Journal of Power Sources*, vol. 225, pp. 172–178, 2013.
- [12] N. Srivastava, S. K. Singh, H. Gupta, D. Meghnani, R. Mishra, R. K. Tiwari, A. Patel, A. Tiwari, and R. K. Singh. “Electrochemical performance of Li-rich NMC cathode material using ionic liquid based blend polymer electrolyte for rechargeable Li-ion batteries.” *Journal of Alloys and Compounds*, vol. 843, p. 155615, 2020.
- [13] F. Wu, M. Wang, Y. Su, L. Bao, and S. Chen. “A novel method for synthesis of layered $\text{LiNi}_{1/3}\text{Mn}_{1/3}\text{Co}_{1/3}\text{O}_2$ as cathode material for lithium-ion battery.” *Journal of Power Sources*, vol. 195, no. 8, pp. 2362–2367, 2010.
- [14] J. Li, H. Li, W. Stone, R. Weber, S. Hy, and J. R. Dahn. “Synthesis of Single Crystal $\text{LiNi}_{0.5}\text{Mn}_{0.3}\text{Co}_{0.2}\text{O}_2$ for Lithium Ion Batteries.” *Journal of The Electrochemical Society*, vol. 164, no. 14, pp. A3529–A3537, 2017.
- [15] C-c. PAN, Y-r. ZHU, Y-c. YANG, H-s. HOU, M-j. JING, W-x. SONG, X-m. YANG, and X.b. JI. “Influences of transition metal on structural and electrochemical proper-ties of $\text{Li}[\text{Ni}_x\text{Co}_y\text{Mn}_z]\text{O}_2$ ($0.6 \leq x \leq 0.8$) cathode materials for lithium-ion batteries.” *Transactions of Nonferrous Metals Society of China (English Edition)*, vol. 26, no. 5, pp. 1396–1402, 2016.
- [16] X. Luo, X. Wang, L. Liao, S. Gamboa, and P. J. Sebastian. “Synthesis and characterization of high tap-density layered $\text{Li}[\text{Ni}_{1/3}\text{Co}_{1/3}\text{Mn}_{1/3}]\text{O}_2$ cathode material via hydroxide co-precipitation.” *Journal of Power Sources*, vol. 158, no. 1, pp. 654–658, 2006.
- [17] H. Jodi, A. Z. Syahrial, Sudaryanto, and E. Kartini. “Synthesis and electrochemical characterization of new $\text{Li}_2\text{O}-\text{P}_2\text{O}_5$ compounds for solid electrolytes.” *International Journal of Technology* vol.8, no. 8, pp. 1516–1524, 2017.
- [18] F. Strauss, T. Bartsch, L. de Biasi, A. Y. Kim, J. Janek, P. Hartmann, and T. Brezesinski. “Impact of cathode material particle size on the capacity of bulk-type all-solid-state batteries.” *ACS Energy Lett.*, vol. 3, no. 4, pp. 992–996, 2018.
- [19] H. Jodi, A. Z. Syahrial., A. Sudjatno, Wahyudianingsih, and E. Kartini. “Sintesis dan kajian perilaku kondukti-vitas komposisi baru elektrolit padat $(\text{Li}_2\text{O})_x(\text{P}_2\text{O}_5)_y$.” *Jurnal Sains Materi Indonesia* vol. 19, no.1, pp. 1–8, 2017
- [20] J. Zheng, P. Yan, L. Estevez, C. Wang, and J. G. Zhang. “Effect of calcination temperature on the electrochemical properties of nickel-rich $\text{LiNi}_{0.76}\text{Mn}_{0.14}\text{Co}_{0.10}\text{O}_2$ cathodes for lithium-ion batteries.” *Nano Energy*, vol. 49, pp. 538–548, 2018.
- [21] H. Jodi, A. Z. Syahrial, Sudaryanto, E. Kartini. “Synthesis and electrochemical characterization of new $\text{Li}_2\text{O}-\text{P}_2\text{O}_5$ compounds for solid electrolytes.” *International Journal of Technology*, vol.8, no. 8, pp. 1516–1524, 2017.
- [22] A. K. Jonscher. “The universal dielectric response.” *Nature*, vol. 267(5613), pp. 673–679, 1997.
- [23] H. Jodi, E. Yulianti, A. Sudjatno, A. Z. Syahrial, and E. Kartini. “Blending effect in $\text{Li}_2\text{O}-\text{P}_2\text{O}_5$ -MMT solid electrolyte and its contribution to conductivity value.” *AIP Conference Proceedings*, vol. 2381, no.1, p. 020025, 2021.

